COMPARISON BETWEEN WIDE BASE SINGLE TIRE AND DUAL TIRES ASSEMBLY BASED ON EXPERIMENTAL PAVEMENT RESPONSE AND PREDICTED DAMAGE

Damien Grellet, Guy Doré, Jean-Pascal Bilodeau, Thomas Gauliard

Damien Grellet
Department of civil engineering, Pavillon Adrien Pouliot
1065, avenue de la Médecine
Québec, QC, Canada
G1V 0A6
Tel.: 418 656-2131 #4876
Email: damien.grellet.1@ulaval.ca

Guy Doré
Professor
Department of civil engineering, Pavillon Adrien Pouliot
1065, avenue de la Médecine
Québec, QC, Canada
G1V 0A6
Tel.: 418 656-2203
Email: guy.dore@gci.ulaval.ca

Jean-Pascal Bilodeau
Research associate
Department of civil engineering, Pavillon Adrien Pouliot
1065, avenue de la Médecine
Québec, QC, Canada
G1V 0A6
Tel. : 418 656-2131 #7242
Email: jean-pascal.bilodeau@gci.ulaval.ca

Thomas Gauliard
Department of civil engineering, Pavillon Adrien Pouliot
1065, avenue de la Médecine
Québec, QC, Canada
G1V 0A6

Word Count:

Body Text	= 4497
Abstract	= 246
Tables 3 x 250	= 750
Figures 8 x 250	= 2000
Total	= 7493

ABSTRACT

Past studies suggest that Wide-Base Single Tires (WBST: 455/55R22.5) induce pavement strains, which are different than duals of similar sizing, some higher and some lower depending on the direction and the location in the pavement. An experimental assessment of strain basins occurring at various positions within the hot-mix asphalt (HMA) layer as well as within the pavement unbound layers was undertaken to further this understanding. The method and results of this assessment along with the pavement damage predicted using available models is presented in this paper. Four failure mechanisms were considered; HMA rutting, bottom-up and top-down fatigue cracking, and structural rutting. Testing was conducted at two sites on a total of four different roads over a range of loads, pressures, and temperatures, using WBST and different sizes of dual tires. Analysis of data showed several critical strain zones near the tire edges and at the tire center. Optic fiber sensors allowed analyzing these phenomena. HMA rutting was calculated considering vertical shear strain near the surface under the edge of the tires. The other failure mechanisms were calculated using maximum strain. The results predict that the WBST tested may induce less damage in the upper part of the HMA layer and more damage considering fatigue cracking and rutting of soils and unbound materials. The data collected was from specific tires and all tests were conducted only under smooth, steady-state rolling conditions. Thus, results should not be generalized to all tires nor extrapolated to predict actual field performance.

INTRODUCTION

By allowing transport of goods and people, and by making possible resource exploitation, roads are essential to social and economic development of regions. On road networks, different axle loading conditions (pressure, load) are imposed on various pavement structures (thickness, materials…). When it comes to truck tires, the potential economic advantage of using wide-base single tire (WBST) instead of dual tires had led trucking industry to develop a new wide base tire which offers improved fuel efficiency, better braking, increased riding comfort and easier handling. It also reduces servicing, maintenance and tire cost, and provides a better pressure control (*1*). Nonetheless, the mechanical response of flexible pavements is directly influenced by the characteristics of the applied traffic loads (tire type, size, internal structure, configuration), and the associated damage may be linked with four main failure mechanisms, which are HMA rutting, top-down and bottom-up fatigue cracking, unbound aggregate and soil (structural) rutting (*2*). Fatigue cracking and subgrade soil rutting have been intensively investigated and are widely incorporated into mechanistic-empirical design procedures. These two mechanisms result from crack initiation at the bottom of HMA associated to repetitive flexure of the layer and from the accumulated permanent deformation occurring due to compressive strain. HMA rutting and top-down cracking are associated with near surface shear and tensile strains and are more difficult to assess due to the difficulty to place strain gauges near the pavement surface. Top down cracking is the result of the propagation of surface initiated longitudinal and/or transverse cracks in HMA layer due to tensile and shear stresses induced near tire edges. HMA rutting occurs in flexible pavement because of the accumulation of small permanent deformations in asphalt concrete due to the combination of densification and repetitive shear deformation (*3*).

Several studies on the pavement induced damages from the use of WBST were conducted in the last few years using field testing and numerical models (*2*)(*4*)(*5*)(*6*)(*7*)(*8*). The main conclusions of these studies vary depending on pavement structure, the pavement damage criteria considered and the climatic conditions. Most of these studies concluded that the 455/55R22.5 WBST causes more damage than conventional dual tires when considering fatigue cracking. Other studies based on numerical modeling concluded that the new generation of WBST reduces rutting and top-down cracking damage (*2*)(*8*). These conclusion have been partly confirmed by field testing (*4*)(*5*)(*8*). Studies suggested that stresses induced near the surface and critical shear strains at shallow depth in the asphalt layer must be included as damage criteria in the mix design methods. Phenomena, other than tensile strains at the bottom of the asphalt concrete layer, should be taken into consideration in the complex mechanical behaviour of pavement bound layers (*5*)(*6*). The tension/compression

responses occurring near the asphalt concrete surface and the shear strains occurring near the tires edges have to be taken into consideration when comparing WBST and dual tires.

Despite the significant advances in pavement analysis made in recent years, the comparison of damage caused by different tire configurations still needs to be verified. The objective of this study is to experimentally quantify the strain differences and predict the pavement damage induced by three specific tires by using strain data collected at various positions within the pavement structure. In this study, the near-surface experimental strains analysis bring new information for the quantification of the overall impact of tire type on the pavement damage. The impact of tire characteristics on flexible pavement structure performances is quantified for the four main failure mechanisms identified. Experimental strain data collected at various positions within the flexible pavement structures of two experimental sites were used and analyzed using appropriate empirical transfer function adapted for each failure mechanism in order to quantify their respective damage ratio.

EXPERIMENT DESCRIPTION

Test sections and material characteristics

To quantify the effect of tire configuration on the different flexible pavement structures, a testing program was performed at two different experimental sites. The tests were carried out on four typical pavement structures, as illustrated on figure 1. The pavement structure for the sections A and B consists of the following layers: 130 and 70 mm thick hot mix asphalt concrete (HMAC) overlying 300 mm of 0/31.5 mm unbound granular base (MG-31.5) and a sandy subgrade soil. The pavement structures for the sections C and D include 100 and 200 mm HMAC overlying 200 mm of 0/20mm granular base (MG-20), 480 mm of 0/112 mm granular subbase (MG-112) and silty sand subgrade. These structures are representative of a wide variety of roads in the Province of Quebec. The asphalt layer identified as:

- HMA N°1 is an dense-graded asphalt concrete 0/10 mm, 70 mm thick (BBSG 0/10) (*10*)
- HMA N°2 is a bituminous mix 0/14 (GB 0/14), 60 mm thick (*10*)
- HMA N°3 is a dense-graded asphalt mix 0/10 mm (ESG-10), 100 mm thick (*5*)
- HMA N°4 is a road base asphalt 0/20 (GB-20), 100 mm thick (*5*)

Test facilities

The tests on sections A and B were conducted at the IFSTTAR's accelerated pavement testing facility near Nantes (France) in 2011. The outdoor test track is a large scale 120-m diameter and 3 m wide circular track, which uses a loading system with a mean radius of 19 m. The device includes four arms, which can be equipped with various load configurations. Each loading module is attached to the extremity of an arm and can move during operation around a mean position to simulate the lateral wandering of the traffic. For of the tests, one arm was equipped with the WBST (455/55R22.5 Xone) and a second one with a dual tire configuration (12.00R20). Four different load levels, varying from 39.2 kN to 63.7 kN were used for the dual tires, while three loads were used for the WBST as shown in table 1. To assess the effect of speed, two or three speeds were considered varying from 32 km/h to 56 km/h. At 39.2 kN, two tire inflation pressures of 690 kPa (100 psi) and 830 kPa (120 psi) were tested. Measurements at the IFSTTAR's facility have been performed exactly at the same time and under the same environment conditions. Because the tests were done during different periods of the day, it was possible to evaluate the impact of the asphalt temperature on the measurements. Several measurements were performed at a cold asphalt temperature (from 16°C to 24.5°C), as well as at a warm temperature (from 24.5°C to 45°C). The tests on sections C and D were conducted at the SERUL (Laval University Experimental Road Site) near Québec City (Canada) in October 2009 and July 2010. The site is an experimental road with a total length of 100 m. The truck used for the testing was loaded at 39.2 kN on WSBT or on dual tire configuration. The first configuration consisted of using conventional dual tires (11R22.5). During the testing days; the tires were changed to WBST. A thermal blanket was installed at the pavement surface over the transducers to minimize the thermal variations. The load and the speed (30km/h) were kept constant during the testing but three tire

inflation pressures were evaluated : 552 kPa (80 psi), 690 kPa (100 psi) and 830 kPa (120 Psi). Table 1 presents the test matrix performed during this project. As indicated, numerous conditions (load, temperature) as well as layer thicknesses were considered.

Instrumentation

To measure vertical strains in the base and in the soil, on sections A and B, resistive deflectometers have been installed in the base layer and in the top 300 mm of the subgrade soil. The instrumentation of the structure B is presented on figure 2. Two retrofit techniques, which allow measuring strains in the upper and lower parts of the asphalt layer have been used on the four sections. These two technologies are: (a) an asphalt concrete core specially trimmed for the installation of strain gages (*5*) and (b) a thin polymeric plate instrumented and fixed inside a saw cut in the asphalt layer. The plate has been designed with poly phenylene sulphide (PPS) to assure mechanical compatibility with the surrounding asphalt concrete (*6*). An epoxy glue is used to fix the instrumentation to the asphalt pavement. This glue has been selected for its chemical and mechanically compatibility with both materials. The core and the plate are instrumented with fiber-optic strain gages using the white-light polarization interferometry technology (*9*). The transducer consists of two optical fibers that are aligned to form an optical Fabry-Perot sensing interferometer. The association of the two instrumentation techniques allows obtaining three-directional strains measurements: longitudinal (X-direction), transversal (Y-direction), and vertical (Z-direction) near the surface (at 20 mm depth). The transverse and longitudinal strains are also obtained at the bottom of HMA layers. This allowed obtaining critical strains at relevant depths of the structures. Temperature transducers were also embedded in HMAC layers to monitor temperature during testing to allow considering the changes in the HMA properties. The measurements were carried out for several lateral tire positions (lateral wandering) in order to obtain more than 50 measurement points. These points are directly under the tires, near the edges and also outside of the tires contact area.

Pavement damage models

To quantify and predict pavement damage caused by different axle configuration, several transfer functions were selected and compared in this study. The critical strains measured with respect to a specific pavement distress type were converted into a number of load repetitions until failure by the following empirical transfer functions:

$$N_F = CK_{F1}\left(\frac{1}{\varepsilon_h}\right)^{K_{F2}}\left(\frac{1}{E}\right)^{K_{F3}} \quad (1)$$

$$N_R = C_R K_{R1}{\varepsilon_v}^{K_{R2}} \quad (2)$$

$$N_{rHMA} = \left(\frac{0.1431}{ae^{(b\tau)}\gamma_e}\right)^{\frac{1}{c}} \quad (3)$$

$$N_{rHMA} = \left(\frac{\mathrm{Rd}}{3.05*10^{-4}}\right)^{\frac{1}{459\gamma_e}} \quad (4)$$

$$N_{rHMA} = \left(\frac{\mathrm{Rd}}{h\varepsilon_{vr}10^{(-3.74938+2.02755\log(T)}}\right)^{1.74} \quad (5)$$

$$N_{TDC} = K_1\left(\frac{1}{\varepsilon_{h_t}}\right)^{K_2}\left(\frac{1}{E}\right)^{K_3} \quad (6)$$

Where:
N_F = number repetition for bottom-up fatigue cracking,
N_R = number repetitions for structural rutting (rut depth=12.5 mm),
N_{rHMA} = number of repetitions for HMA rutting (failure rut depth = Rd),
N_{TDC} = number of repetitions for top-down cracking,
ε_h = tensile strain at the bottom of the HMA layers,
ε_{ht} = surface tensile strain,
ε_v = vertical compressive strain at the top of base/soil,

ε_{vr} = vertical compressive strain near surface of HMA,
γ_e = shear strain near surface of HMA.
Each transfer function depends on the material properties:
E = modulus of HMA,
T = pavement temperature,
h = HMA thickness (mm),
C = fatigue correction factor,
C_R = rutting correction factor,
$K_{F1}, K_{F2}, K_{F3}, K_{R1}, K_{R2}, K_1, K_2, K_3, a, b\ and\ c$ are experimental regression model constants .
The coefficients used in each transfer function are given in table 2. Complex modulus tests have been performed on the bituminous materials (*10*) to calculate the asphalt modulus at specific frequency and temperature using the Huet-Sayegh model (*17*)(*18*).

RESULTS AND DATA ANALYSIS

Pavement response validation

Several validation tests were done to ensure the high level of quality of measured strains. First, testing was conducted shortly after installation of the instrumentation to minimize the risk that measurements be influenced by pavement damage (cracking). Then, duplicate gauges of each type of instrument have been installed and repeatability of individual gauges has been determined for each condition of the experimental program. The strains measured with two independent sensors submitted to similar loading conditions, were compared to make sure similar shape and amplitudes were obtained. Finally, the signal shape was compared to measurements documented in other field studies and compared to signals obtained by simulations with the *ViscoRoute 2.0*© software (*19*) using a viscoelastic model. This analyze concluded that the use of optic fiber sensors allowed to adequately characterize the strains occurring within the layer (*10*).

Value and location of the critical strain in the structure

Data collected during the experimental program were used to produce strain basins. Under each type of tires, the basin was determined by performing measurements at progressively increasing tire offset (Y position) as presented in figure 2. Examples of the strain basin slope (ε_{yy} and ε_{zz}) near HMA surface can be observed on the figure 3, as well as the transversal strain basin (ε_{yy}) at the bottom of HMA layer. The coordinate Y=0 mm, is the center of the tire. The sign convention is positive for extension (tensile strain) and negative for contraction (compressive strain). Satisfying strain basins were obtained and data analysis and interpolation allowed assessing the critical strain value specific to the deterioration mechanisms considered. At the bottom of the layer, an interpolation curve was used and the maximum values of the strain basin were considered for calculation. The tensile strain considered is directly under the center of the tire. As illustrated, the maximum strain caused by WBST is higher than the ones induced by dual tires. For the top-down cracking, the maximum tensile strain of the transversal strain basin (ε_{yy}) near the tire edges was considered. The results are also slightly more scattered near the surface because of the higher signal/noise ratio and the greater effect of the tire tread (*10*).

For the shear strain near the surface, additional analysis of the experimental data was needed. Studies have shown that maximum vertical shear strain in HMA layer is typically measured at a depth of approximately 2 cm (*2*). The fiber optic vertical strain sensors were thus located at that depth for the tests. This critical depth may vary with the pavement thickness. In order to calculate vertical shear strain under tire edges, the method used in this study involved the determination of the vertical strain basin slopes. As illustrated in figure 3, an interpolation of the vertical strain basin (ε_{zz}) was used and the maximum slopes of the strain basin under tire edges were calculated. The method has been applied for all experimental conditions (pavement structures under different loading, temperature, speed and tire pressure). Then, using theoretical loading simulations computed by *ViscoRoute2.0*© software , a

relationship between vertical strain basin slopes and shear strain was obtained. The relationship is expressed as:

$$\gamma = (aT^2 + bT + c) * \Delta\varepsilon_{zz} \quad (7)$$

where
$\boldsymbol{\gamma}$= shear strain,
T = asphalt temperature,
$\Delta\boldsymbol{\varepsilon_{zz}}$ = maximum slope under tire edges,
a, b and c are regression coefficients.
The regression coefficients obtained for each experimental conditions are given in table 3.

Strain ratio

For each type of strain, the strain ratio is defined as the maximum strain induced by the WBST divided by the maximum strain induced by the dual tires. The results, summarize on the figure 4, show the influence of the asphalt thickness and the temperature on the different ratios.

DAMAGE RATIO

The damage ratio for each failure mechanism was calculated using equation (8). Pavement life ratios allow for a comparison between the tire configurations on the basis of pavement damage as calculated using equations 1 to 6. A ratio above 1 indicates that pavements will experience more damage if only WBST were used.

$$DR_i = \frac{N_{Dual\ tires}}{N_{WBST}} \quad (8)$$

Where
$\boldsymbol{DR_i}$= damage ratio for the considered failure mechanism i.
$\boldsymbol{N_{Dual\ tires}}$= number of cycles to failure for dual tires,
$\boldsymbol{N_{WBST}}$= number of cycles to failure for WBST

Fatigue cracking

Results presented in figure 4, suggest that the WBST would cause between 1.05 and 1.45 more strain at the bottom of the asphalt layer than the dual tire assembly. The increase in strain results in more fatigue damage to the pavement. Figure 5 presents the fatigue damage ratios calculated with five different prediction models. This analysis was done considering two cases: stationary and wandering loads. The stationary case considers the highest strain value to predict pavement life. The wandering case takes into account the strain basin's shape and represents more closely real traffic condition. The wander is generated using a tire position variation function with a standard deviation of 150 mm. From these results, for all testing conditions, the WBST is more damaging than dual tires for bottom-up fatigue cracking. It is evident from these results that the decrease in HMA thickness results in less damage ratio and this ratio tends to be lower for warm temperatures. With respect to the effect of wander, it appears that the damage ratio increased with the application of the wander. The overall tire width will have a bigger influence on the strain basin for a weak structure (structure B, C and A at warm temperature). The damage ratio increases by a factor 1.5 for these structures when considering the wandering loading. On the other hand, the damage ratios only increase by 1.05 for the structure D. The differences found between the damage models used to seem to be more important for thicker structures, and the standard deviation between models is up to 0.96 in the most critical conditions. These differences can be explained by the fact that these empirical models were generally developed for specific site conditions and characteristics. However, in general, the models agree quite satisfactorily on the effect of temperature and HMA thickness, as the trends observed are mostly the same regardless of the models considered for the analysis.

Permanent deformation of soil and granular materials (structural rutting)

As presented in figure 4, the vertical compressive strains induced by WBST are greater on the top of the base layer and of the soil. The damage ratio has been calculated using four different damage predictions models (table 2). Figure 6 presents the ratios for secondary rutting at the top of the granular base as well as the rutting of the subgrade soil. The analysis was also done using the stationary and the wandering loading conditions as described above. For all testing conditions, WBST is more damaging than the dual-tire assembly, as ratios higher than one are observed. In general, the damage ratios for structural rutting are 21% lower in average using the wander method for calculation instead of the stationary loading approach. Moreover, it is noticed that damage ratio for rutting seems to be higher on thinner structures and at higher temperatures, especially at the top of the subgrade soil. Some differences are observed between the computed results between the models considered, but a good agreement is found between each model when it comes to the effect of HMA thickness or temperature.

HMA rutting and top-down cracking

As presented in figure 4, it appears that near the surface, the dual tire assembly caused more shear strain at the edges of the tires and more compressive vertical strains. On the other hand, the tensile transversal strains at the edges of the tires are higher for the WBST. Figure 7 presents the results of the damage ratios calculated for HMA rutting based on the maximum compressive strain (model 12). From these results, the WBST is less damaging than the dual tire in stationary loading conditions but more damaging considering wander loading for all testing conditions. Based on the maximum transversal tensile strain (model 13), the damage ratios calculated for top-down cracking is above 1 indicated that WBST is more damage. HMA rutting was determined using the model 10 and 11 based on the shear strain near the edge of the tires. At each specific season, the shear strain associated with the temperature is used to calculate the cumulative rutting. The damage ratios based on model 10 are 0.89 (structure A) and 0.82 (structure B). Based on model 11, the ratios become respectively to 0.84 and 0.80. The lateral wandering of the tires has been considered in the seasonal analysis.

DISCUSSION

At the bottom of the asphalt layer, significant strain basin differences were measured between the two tire types. It can be noticed that near the surface, the dual tire presents four critical areas (at each tire edge) with high-tensile strain and shear strain. The WBST presents only two areas. The empirical transfer functions used in the study only considered the critical strain levels. Other shape parameters characterizing a pavement response (strain basin, three direction strain distribution under the tire) may have a non-negligible influence on the fatigue life of the asphalt. Researchers still investigate the cause of top-down cracking. Considering the strain level, shear strain may have a bigger impact than tensile strain on the initiation of the damage near the surface of the layer. The proposed damage ratios are based on the pavement response, and they need to be correlated with field performance observed at a full scale accelerated pavement testing facility.

An aspect of this study was to measure the impact of a differential tire inflation pressure for a dual tire. As a matter of fact, studies have shown that approximately 7.08% of all tires are under inflated by 138 kPa (20 psi) or more and only 44.15% of all tires are within ±34.5 kPa (5 psi) of their target pressure (*20*). Tests have been conducted on the section D at a temperature of 23°C. The dual tire was loaded at 39.2kN and tests were performed at 30km/h for two configurations: (a) both tires were inflated at 690 kPa and (b) a differential pressure was imposed. On tire was inflated at 550 kPa and the other one at 690 kPa. Figure 8 presents the implication of the improper inflation pressure of dual tires relative to the strain ratios with the WBST. Results have identified a decrease from 1.44 to 1.29 of the transversal strain ratio at the bottom of the HMA leading to a decrease of the fatigue damage ratio from 3.3 to 2.3 (using model 1). The results suggest that improper inflation pressure of dual tires would cause more transversal strain near the surface of the HMA than the WBST. As illustrated, the

ratio decrease from 1.08 to 0.94 leading to a decrease of the rutting damage ratio from 1.33 to 0.79 (using model 13 with stationary load).

CONCLUSIONS

The objective of this study was to quantify the strain differences and predict the pavement damage induced by three specific WBST and dual tires of similar and dissimilar sizing by using experimental strain data collected at various positions within the pavement structure. Strain measurements were taken under various experimental conditions to obtain the critical strain level and location under the tire. For different type of strains, strain ratios were calculated to compare the relative response of the pavement structure under the two types of tires in different testing conditions. The damage ratios between the two tire types were calculated for four failure mechanisms. Under the conditions evaluated, the particular WBST tires studied may cause more damage versus the conventional dual tires considering fatigue cracking and rutting of soils, but near the surface of the layers, the WBST may reduce the damage since they induce a reduction of the shear and vertical compressive strains, with a rise of the tensile strain near the tire edges. The complexity of the strain near the surface suggests that detailed characterization of the causes of damage is required for prediction of pavement performance. As the data was acquired under idealized and limited conditions, results should not be generalized or extrapolated to anticipate actual field behaviour.

AKNOWLEDGEMENTS

The authors wish to thank the National Sciences and Engineering Research Council as well as the partners of the i3C NSERC industrial research Chair, and more specifically Michelin Canada and the Quebec Ministry of Transportation for their financial and technical contribution. The authors wish also wish to express their full gratitude to IFSTTAR and its fatigue carrousel research crew, and more specifically Gilles Coirier, Thierry Gouy, Jean-Pierre Kerzreho and Stéphane Trichet for their close cooperation throughout this research project.

REFERENCES

1. Al-Qadi, I. and M. Elseifi, 2007, New Generation of Wide-Base Tires: Impact on Trucking Operations, Environment, and Pavements. In: *Transportation Research Record: Journal of the Transportation Research Board*. No. 2008, Transportation Research Board, Washington D.C., 2007, pp. 100-109.
2. Al-Qadi, I.L., H. Wang, *Evaluation of Pavement Damage Due to New Tire Designs*. Research Report ICT-09-048, Illinois Center for Transportation, University of Illinois at Urbana-Champaign, 2009.
3. Selvaraj, S.I., *Development of flexible pavement rut prediction models from the NCAT test track structural study sections data*, Dissertation submitted to the Graduate Faculty of Auburn University, UMI 3265520, 2007.
4. Pierre, P., G. Doré and J.-P. Bilodeau, Strains at shallow depth in bound surfacing materials. In Proceedings of the *10th International Conference on Asphalt Pavement*, Québec, Canada. Vol. 2, 12-17 August 2006, pp 1491-1503.
5. Grellet, D., G. Doré and J.-P. Bilodeau, Comparative study on the impact of wide base tires and dual tires on the strains occurring within flexible pavements asphalt concrete surface course. *Canadian Journal of Civil Engineering*, Volume 39, Number 5, 2012, pp. 526-535.
6. Grellet, D., G. Doré, and J.-P. Bilodeau, Effect of tire type on strains occurring in asphalt concrete layers. In Proceedings of the *11th International Conference on Asphalt Pavements*, August 1st to 6th, Nagoya, Japan. Vol. 2, 2010, pp 985-994.
7. Prophete, F.: Effect of Different Types of Tires on Pavements. . In Proceedings of the *10th International Conference on Asphalt Pavement*, 12-17 Québec, Canada, Vol. 2, August 2006, pp1186-1197.
8. Green, J., U. Toros, S. Kim, T. Byron and B. Choubane, *Impact of wide-base single tires on pavement damage*. Research report FL/DOT/SMO/09-528, Florida Department of Transportation, 2009.
9. Doré, G., G. Duplain and P. Pierre, Monitoring mechanical response of in service pavements using retrofitted fiber optic sensors. In: Proc of the Intern. *Conf. on the Advanced Charact. of Pavement and Soil Eng. Materials*, Athens, Greece, 2007, pp 883-891, ISBN 978-0-415-44882-6.
10. Grellet, D., G. Doré, J.-P. Kerzreho, J.-M. Piau, A. Chabot, P. Hornych, Experimental and theoretical investigation of three dimensional strain occurring near the surface in asphalt concrete layers. In Proceedings of the *7th RILEM International Conference on cracking in pavements*, Delft, The Netherlands, 2012, pp 1017-1027, ISBN 978-94-007-4565-0.
11. MnPAVE 6.100 User's Guide: *Mn/DOT Flexible Pavement design: Mechanistic-Empirical Method*, Minnesota Department of Transportation, ©2000-2011, pp.34.
12. ARA, Inc., Eres Consultants Division. *Guide for Mechanistic–Empirical Pavement Design of New and Rehabilitated Pavement Structures*. Final Report, NCHRP 1-37A. Transportation Research Board of the National Academies, Washington, D.C., 2004.
13. Timm, D. H., and D. E. Newcomb, Calibration of Flexible Pavement Performance Equations for Minnesota Road Research Project. In *Transportation Research Record: Journal of the Transportation Research Board*, No. 1853, Transportation Research Board of the National Academies, Washington, D.C., 2003, pp. 134–142.
14. Al-Qadi, I.L., M. Elseifi and P.J. Yoo, *Pavement Damage Due to Different Tires and Vehicle Configuration.* Final Report Submitted to Michelin Americas Research and Development Corporation. Virginia Tech Transportation Institute, 2004, 80 p.
15. Monismith, C.L., L. Popescu, and J.T. Harvey, Rut Depth Estimation for Mechanistic-Empirical Pavement Design Using Simple Shear Test Results. *Journal of Association of Asphalt Paving Technologists*, Vol.75, 2006, 41p.
16. Deacon, J.A., J.T. Harvey, I.Guada, L. Popescu, C.L. Monismith, Analytically Based Approach to Rutting Prediction. In *Transportation Research Record: Journal of the Transportation Research Board*, No. 1806, Transportation Research Board of the National Academies, Washington, D.C., 2002, pp. 9-18.

17. Huet C. *Etude par une méthode d'impédance du comportement viscoélastique des matériaux hydrocarbonés*. Ph.D dissertation, Université de Paris, 1963
18. Sayegh G., *Contribution à l'étude des propriétés viscoélastiques des bitumes purs et des bétons bitumineux.* Ph.D dissertation, Faculté Sciences de Paris, 1965
19. Chabot, A., O. Chupin, L. Deloffre and D. Duhamel, ViscoRoute 2.0: a tool for the simulation of moving load effects on asphalt pavement. *RMPD Special Issue on Recent Advances in Num. Simul. of Pavements*, 11 (2), 2010, pp. 227-250.
20. Kreeb, R. M., B.T. Nicosia, and P.J. Fisher, *Commercial Vehicle Tire Condition Sensors*, Report FMCSA-PSV-04-002, United States Department of Transportation, Washington, DC, 2003.

LIST OF TABLES

LIST OF FIGURES

TABLE 1 Number of analysed cases for each combination of loads and tire types

	Section A				Section B				Section C		Section D	
Tire	D.T.		WBST		D.T.		WBST		D.T.	WBST	D.T.	WBST
T°	Cold	Warm	Cold	Warm	Cold	Warm	Cold	Warm	Cold	Cold	Warm	Warm
39.2 kN	2	1	2	1	2	2	2	2	3	3	3	2
49.0 kN	3	3	3	3	2	2	2	2	-	-	-	-
56.9 kN	1	1	1	1	1	1	1	1	-	-	-	-
63.7 kN	1	1	-	-	1	2	-	-	-	-	-	-

D.T.=Dual tires, WBST= Wide-base single tire, - = No experimental data
Cold: T° from 16°C to 24.5°C. Warm: T° from 24.5°C to 45°C.

TABLE 2 Coefficient of the pavement damage models

Fatigue						
Model	Equation	Reference	C	K_{F1}	K_{F2}	K_{F3}
1	(1)	(*11*)	0.314	1.2	3.291	0.854
2	(1)	(*2*)	1	2.65×10^{-9}	4.0	0
3	(1)	(*12*)	0.314	1.0841	3.9492	1.281
4	(1)	(*13*)	1	2.83×10^{-6}	3.148	0
5	(1)	(*7*)	1	$1,23281 \times 10^{-6}$	3.29	0
Structural rutting						
Model	Equation	Reference	C_R	K_{R1}	K_{R2}	
6	(2)	(*11*)	1.39	0.0261	-2.35	
7	(2)	(*14*)	1	1.077×10^{-8}	-4.483	
8	(2)	(*11*)	1	1.110×10^{-8}	-3.949	
9	(2)	(*15*)	1	1.365×10^{-9}	-4.477	
HMA rutting						
Model	Equation	Reference	a	b	c	
10	(3)	(*16*)	2.114	0.04	0.124	
11	(4)	(*3*)	-	-	-	
12	(5)	(*14*)	-	-	-	
Top down cracking						
Model	Equation	Reference	K_1	K_2	K_3	
13	(6)	(*2*)	1.7885×10^{-5}	3.9492	1.281	

- = Not applicable

TABLE 3 Coefficient of the equation (7) for different structure and conditions

Structure and conditions	a	b	c	R^2
A at 42 km/h	-0.0180	1.226	11.578	0.978
A at 32km/h and 17.1°C	0	0	50.533	1
A at 32km/h and 19.7°C	0	0	28.658	1
A at 56km/h and 18.8°C	0	0	27.317	1
B at 42 km/h	-0.0435	2.180	26.051	0.995
B at 32km/h and 24.9°C	0	0	52.241	1
B at 32km/h and 24.3°C	0	0	52.115	1
B at 56km/h and 18.9°C	0	0	50.533	1
C at 30 km/h	-0.0052	0.368	25.064	0.998
D at 30 km/h	0	0.278	15.368	0.999

Equation (7): $\gamma = (aT^2 + bT + c) * \Delta\varepsilon_{zz}$

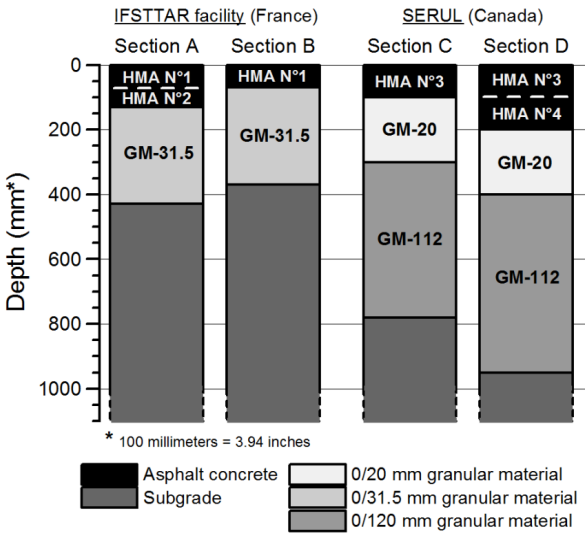

FIGURE 1 Pavement structure of the four analysed road sections.

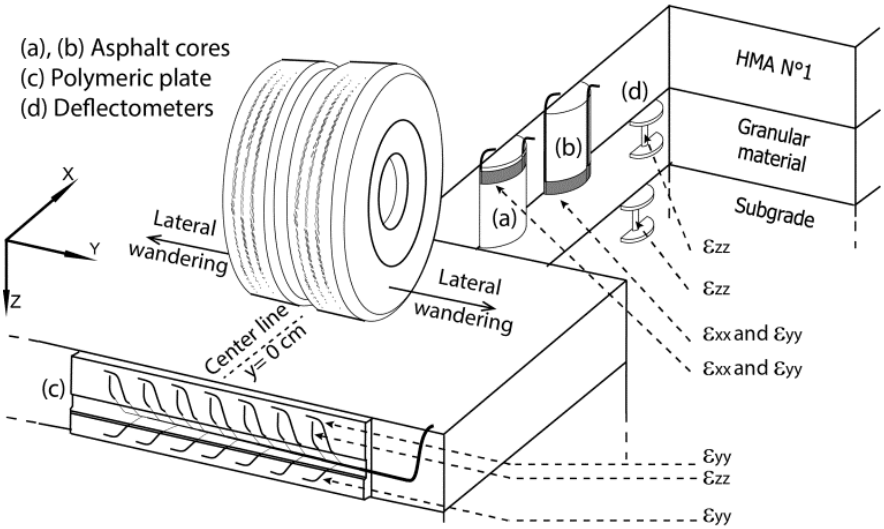

FIGURE 2 Configuration and instrumentation of the structure B

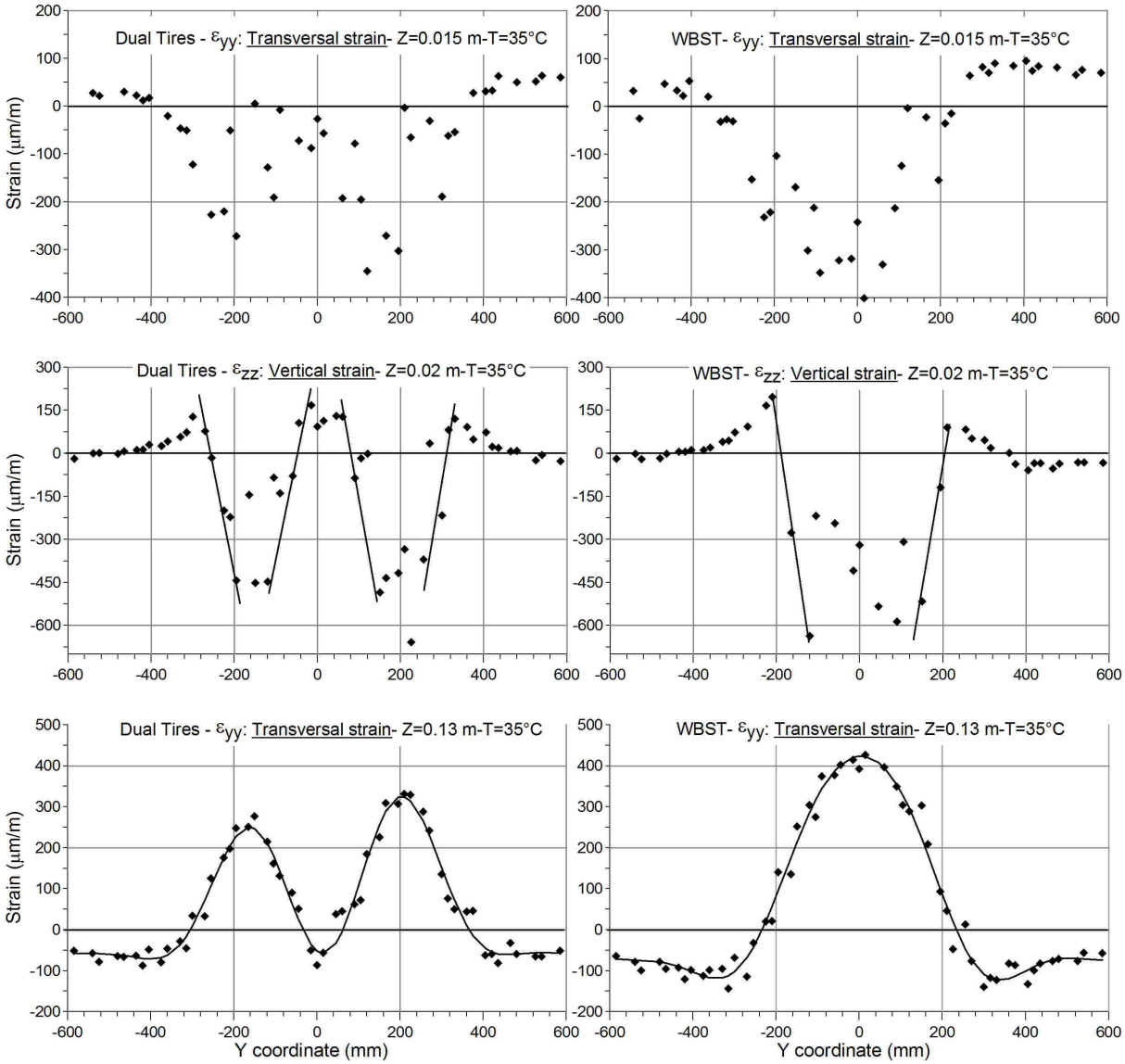

FIGURE 3 Strain basin under the two tire configurations for section A (at 42 km/h, 5 tons, 120 Psi and 35°C).

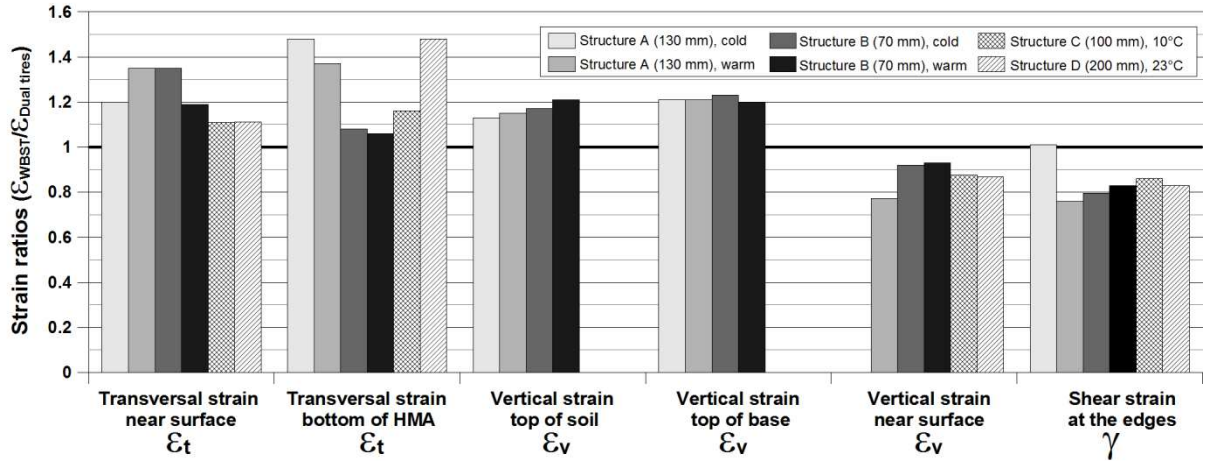

FIGURE 4 Synthesis of critical strain ratios (strain for WBST/strain for dual tires).

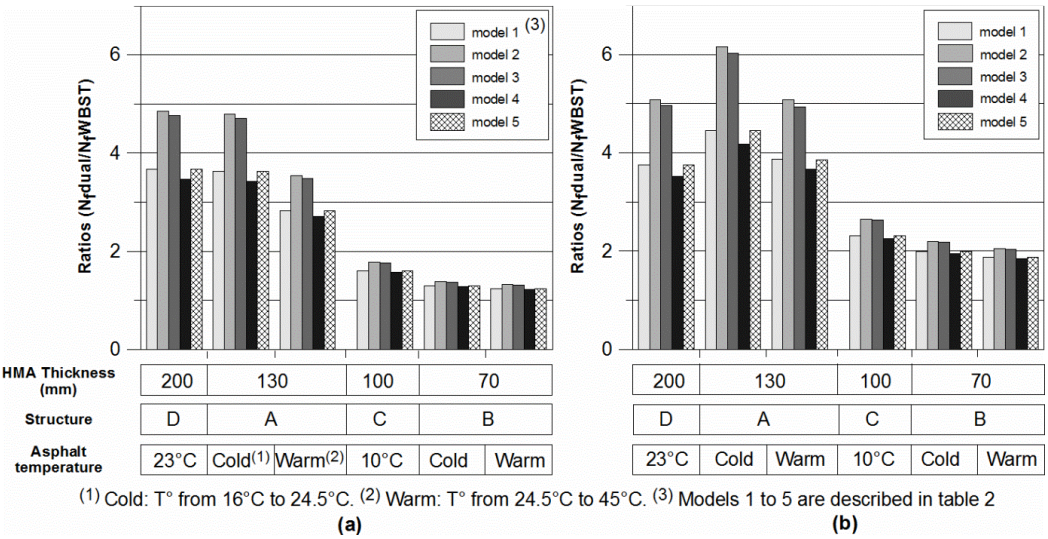

FIGURE 5 Pavement fatigue life ratios between the two tire configurations with: (a) stationary loading, and (b) wandering loading.

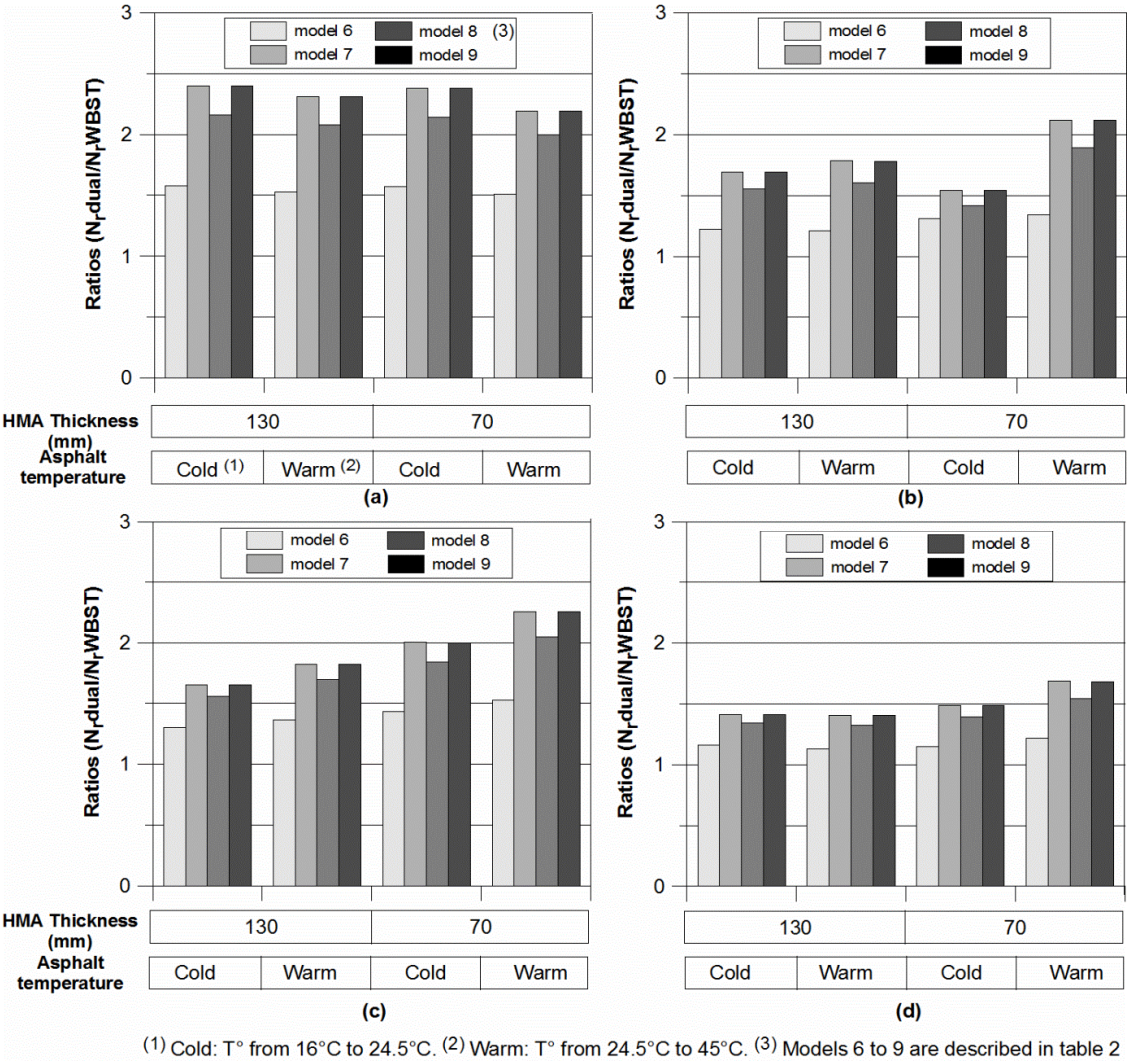

(1) Cold: T° from 16°C to 24.5°C. (2) Warm: T° from 24.5°C to 45°C. (3) Models 6 to 9 are described in table 2

FIGURE 6 Pavement rutting life ratios between the two tire configurations with: (a) stationary loading at top of the base, (b) wandering loading at top of the base, (c) stationary loading at top of soil, (d) wandering loading at top of the soil.

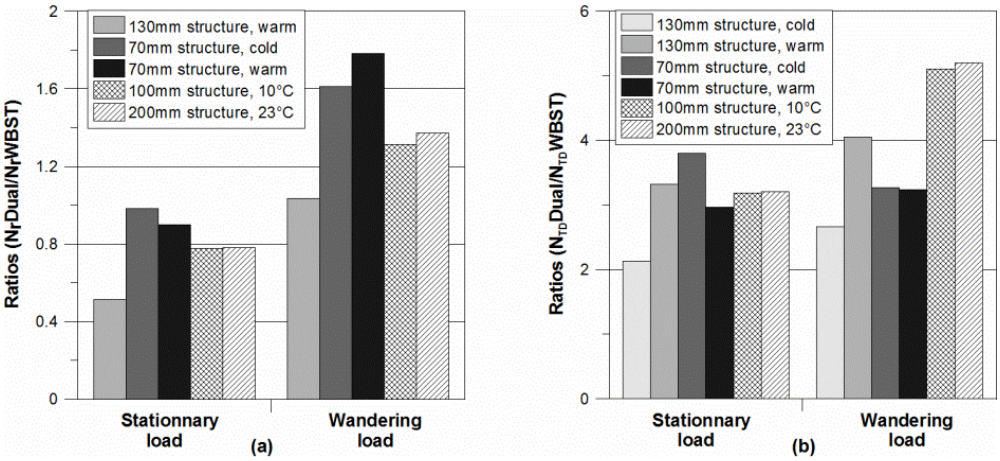

FIGURE 7 (a) HMA rutting life ratios between the two tire configurations (model 12 of table 2); (b) pavement top-down cracking life ratios between the two tire configurations (model 13 of table 2).

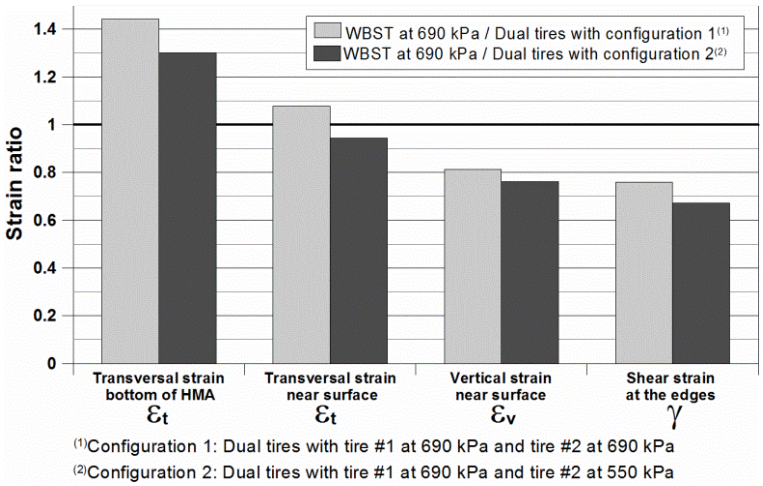

FIGURE 8 Synthesis of critical strain ratios for structure D at 23°C with differential tire pressure